U.S.NRC
United States Nuclear Regulatory Commission
Protecting People and the Environment

Technical Letter Report

TLR-RES/DE/CIB-2021-02

Effect of Crack Face Pressure Distribution on Crack Opening Displacements and Associated Leak Rates

Date:

September 18, 2020

Prepared in response to Task 3 in User Need Request NRR-2020-004, by:

E. Twombly
Engineering Mechanics Corporation of Columbus

F.W. Brust
Engineering Mechanics Corporation of Columbus

NRC Project Manager:

Jay Wallace
Materials Engineer
Component Integrity Branch

Division of Engineering
Office of Nuclear Regulatory Research
U.S. Nuclear Regulatory Commission
Washington, DC 20555–0001

DISCLAIMER

This report does not contain or imply legally binding requirements. Nor does this report establish or modify any regulatory guidance or positions of the U.S. Nuclear Regulatory Commission and is not binding on the Commission.

Final Report On

Effect of Crack Face Pressure Distribution on Crack Opening Displacements and Associated Leak Rates

U.S. Nuclear Regulatory Commission
Prime Contract No.: NRC-HQ-25-14-E-0004
NUMARK Job No. 4409, Task Order 9
Emc^2 Project Number: 17-G121-01
As a Subcontractor to NUMARK Associates, Inc.

to

U.S. Nuclear Regulatory Commission
Washington, D.C. 20555-0001
by

E. Twombly, F.W. Brust

Engineering Mechanics Corporation of Columbus
3518 Riverside Drive, Suite 202
Columbus, OH 43221
Phone/Fax (614) 459-3200/6800

September 18, 2020

As a Subcontractor to
NUMARK Associates, Inc.
1220 19th Street, NW, Suite 500
Washington, DC 20036

Executive Summary

Accurate estimation of leakage rate of a pipe with a through-wall crack is fundamental to the concept of Leak-Before-Break (LBB). A critical input parameter for estimating leak rate is the crack opening displacement (COD) that results from service loads in pipes. Other factors, such as weld residual stress and crack face pressure (CFP) distribution, also affect COD, thus leak rate.

This report presents the results of a literature survey of appropriate two-phase leakage models that can be used to estimate CFP distribution. Three CFP distributions for were selected for evaluation. The effect of each of the CFD distributions on COD was evaluated using finite element analysis, and the leakage rate was estimated using the LEAPOR leakage code. The results show that the choice of CFP distribution is important for enhancing the fidelity of the COD calculations and can be critical for leak rate estimation, particularly for long cracks.

ACKNOWLEDGEMENTS

The authors gratefully acknowledge the helpful comments provided by the NRC staff during the preparation of this report. In particular, the extensive comments, edits, and contributions from the Office of Nuclear Reactor Regulation and the Component Integrity Branch are gratefully appreciated.

Effect of Crack Face Pressure Distribution on Crack Opening Displacements and Associated Leak Rates

E. Twombly, F.W. Brust

1. Introduction

When a surface crack breaks through to become a through-wall crack leakage begins. Leakage is typically predicted using either the SQUIRT code or the newer LEAPOR module, which produces results similar to SQUIRT. The pressure along the crack faces within xLPR is assumed to be half the operation pressure. In reality, the pressure along the crack face is rather complicated and this may affect leak rates, especially for tortuous PWSCC crack paths. Crack face pressure effects on COD at the piping inside diameter and outside diameter will be developed and evaluated for a typical Westinghouse 4-loop plant hot leg nominal piping size. The first part of this report involves attempting to estimate the pressure distribution across the crack face for a simple fluid model within ABAQUS and other computational fluid dynamics (CFD) codes. The second part of this report examines the effect of varying pressure distribution along the crack face along on the crack opening displacement (COD) and associated leakage rates.

2. Crack Face Pressure Distribution and CFD

In order to determine the pressure effect of the fluid on the crack face, a simple CFD analysis was attempted using ABAQUS. In recent releases the CFD module in ABAQUS has been separated from the other solvers and a different license is required to use the CFD module, however, older versions of ABAQUS can still be used to perform a CFD analysis with a standard license. Therefore, initial investigations of the crack face pressure distribution were done using the ABAQUS 2016 CFD solver. A simple fluid mesh, which consists of the fluid in a pipe and the fluid through a through wall crack, was created and is shown in Figure 1. The pipe is a 16-inch diameter pipe with 1.5 inch thickness and the crack is 1 inch long with a COD of 0.2 inches. Although the analysis will eventually use a hot leg PWR piping nominal size, the pipe and crack size was chosen for this initial exploratory analysis with consideration given for the mesh size.

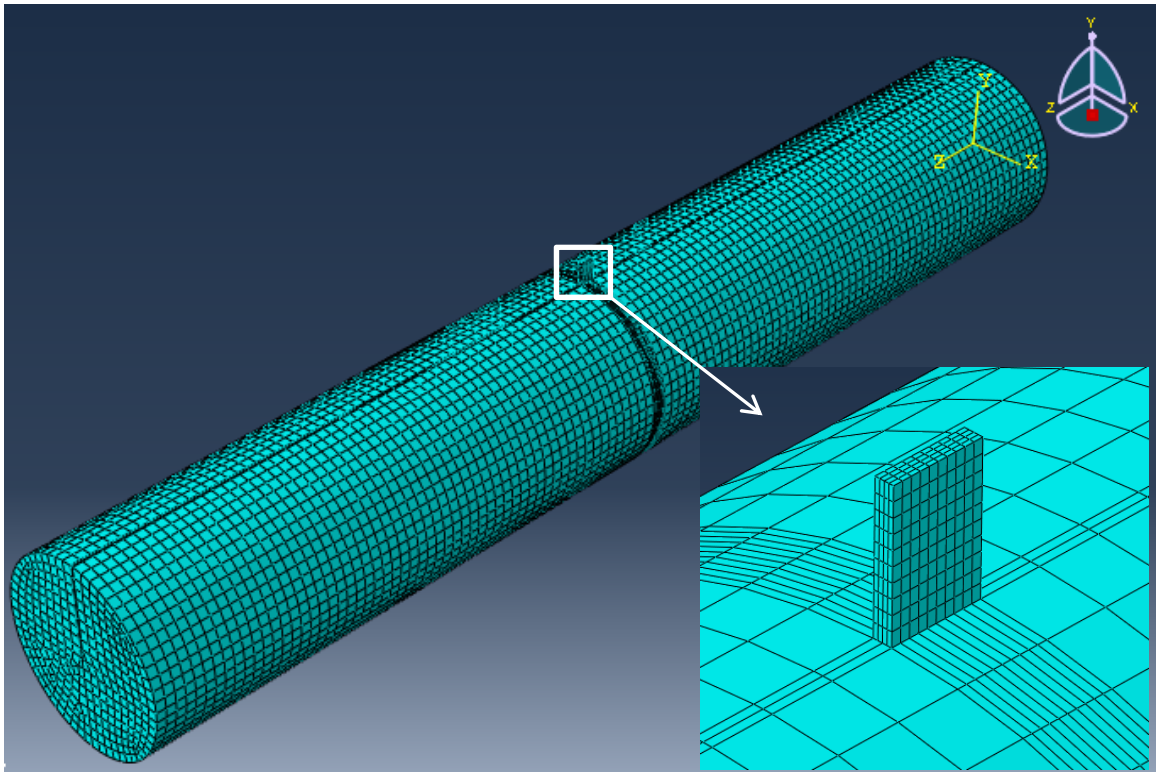

Figure 1: Initial ABAQUS 2016 CFD mesh for flow through a crack

As can be seen in the inset of Figure 1, the crack shape is rectangular rather than the typical elliptical shape that is used in leakage rate calculations. Again, this was a simplification of the mesh that was made for this initial exploratory analysis. This analysis used initial conditions, including the density of water in its liquid state at standard temperature and pressure (STP) and also its kinematic viscosity at STP. The model also uses the Spalart-Allmaras turbulence model [1]. The initial velocity is set to zero. In the first step the boundary conditions are set to have the ends of the fluid in the pipe with a pressure of 2250 psi as well as the inner diameter of the crack area. The outer diameter of the crack area has a pressure set to 14.7 psi (atmospheric pressure). The inner diameter pipe fluid surface has a no slip wall condition boundary condition. Initial results of this analysis are shown in Figure 2.

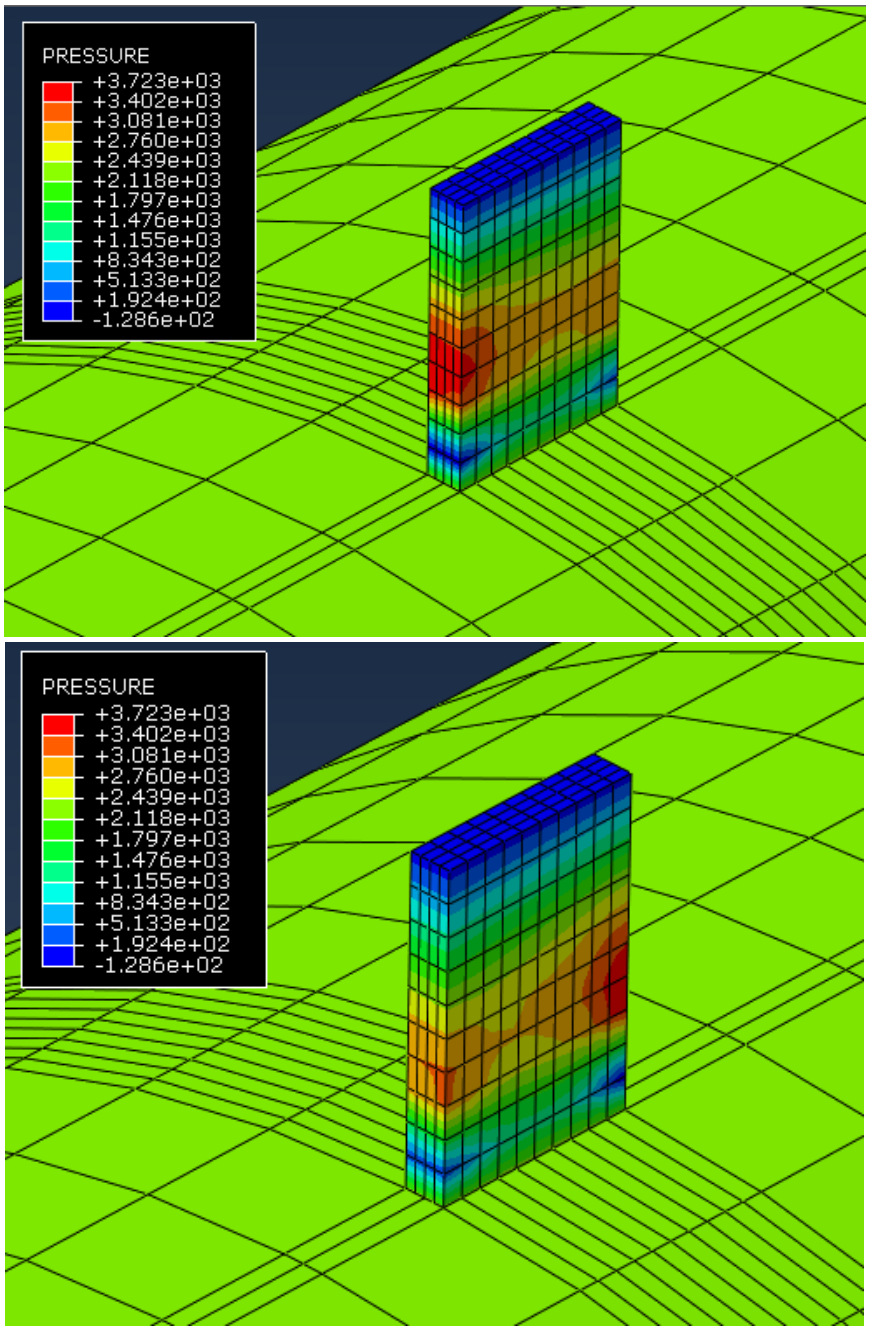

Figure 2: CFD exploratory analysis results for pressure distribution (bottom image is 180° rotation about y-axis)

The pressure distribution shown in Figure 2 leads to a couple of unexpected observations. The first is that when the top and bottom images are compared (the bottom image is just a 180° rotation about the y-axis from the top image – see Figure 1 for axis definition), it is seen that the pressure distribution is not symmetric. The second observation is that the pressure at the ID is 2250 psi and at the OD is 14.7 psi but the maximum pressure at the midpoint of the crack is about 3600 psi. This is not just an unexpected increase in the pressure over the flow path length, but a physically unrealistic result.

Upon further investigation of these results it was discovered that although the job completed, it did not converge to a solution. Therefore the results presented in Figure 2 were showing divergence. The pressure profile right before the solution began to diverge is shown in Figure 3. These results are much more in line with the expectation of how the pressure gradients across the flow path look.

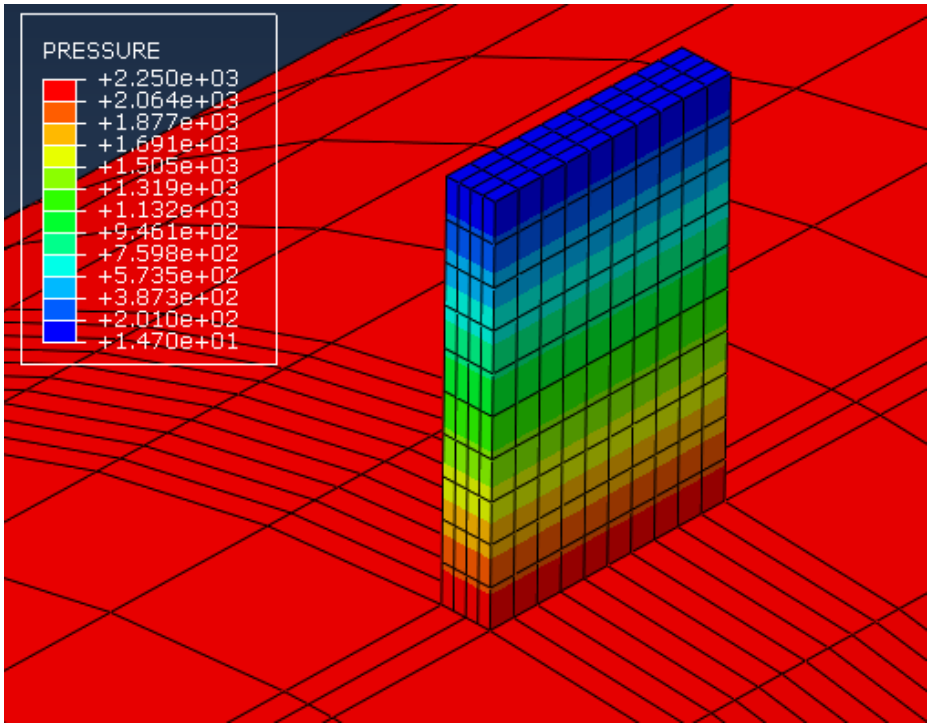

Figure 3: Pressure gradient results for the initial analysis right before divergence

The initial exploratory analysis shows that a CFD analysis to investigate the pressure distribution across the flow path through a crack can be performed, however, accurate inputs are key to obtaining converged, and realistic results. In this initial exploratory analysis, many simplifications were made regarding the inputs, most notably, using constant, temperature-independent values for the density, specific heat and viscosity fluid properties. Therefore, the analysis was updated with the temperature-dependent properties for specific heat and viscosity shown in Table 1. It should be noted that the simple CFD model in ABAQUS does not have a two phase flow model, thus the properties for water are used in this table. This module does not have a way to use steam tables. If the analysis is able to converge then an approximation to model two phase flow results would be to use steam properties and assume an equilibrium condition much like the Henry Fauske model does. In order to fully incorporate a two phase flow model a more robust CFD solution would be necessary.

Table 1: Temperature Dependent Water Properties Used [2], [3]

Temperature (°F)	Specific Heat (Btu/lb_m°F)	Viscosity ($lb_f \cdot s/ft^2$)
32	1.01	3.7414E-5
60	1	2.3405E-5
120	1	1.1652E-5
180	1	7.192E-6
240	1.01	5.05E-6
300	1.03	3.84E-6
350	1.05	3.202E-6
400	1.08	2.75E-6
450	1.11	2.404E-6
500	1.19	2.126E-6
550	1.29	1.888E-6
600	1.50	1.673E-6
650	2.09	1.438E-6
675	3.19	1.292E-6

Even with the temperature-dependent fluid properties the analysis was not able to converge. The interim results are shown in Figure 4. These interim results show the same trend for the pressure distribution as the initial analysis with temperature independent fluid properties.

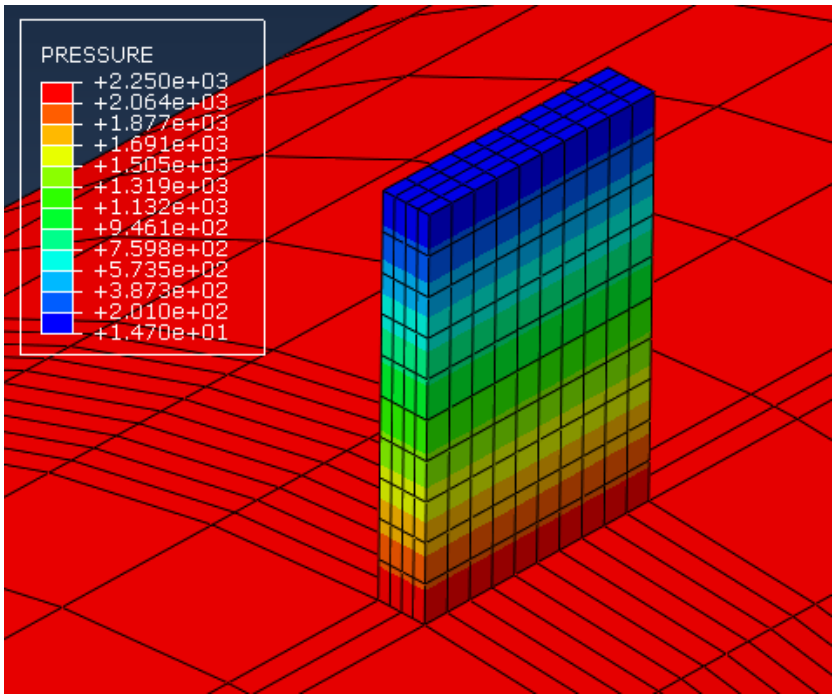

Figure 4: Results immediately before divergence for temperature dependent fluid properties

The analyses do not take an extremely long time to run, on the order of a couple hours even if there are convergence issues. Analyses were performed to determine if the pipe mesh was necessary, or if the problem could be modeled using only the crack mesh. If the pipe mesh could be excluded without loss of accuracy in the results, then not only would the analysis run faster, but it would be possible to refine the crack mesh with less impact on the computational time. In order to ascertain this, two analyses were

performed: one with the pipe mesh included and one without. Both analyses had the exact same inputs. The results from both of these analyses were exactly the same. Therefore, the pipe mesh was excluded from the remainder of the analysis.

Once it was determined that the pipe mesh was not necessary, resolving the convergence issue was addressed. Another significant assumption is that default parameters for the turbulence model were used. Therefore, an analysis where turbulence was not modeled was run. The results for this analysis are shown in Figure 5. Although this solution also diverged, it was able to get closer to a solution than the case where a turbulence model was defined. It is noted, however, that the trend for the pressure distribution is the same as the analysis in which turbulence is included.

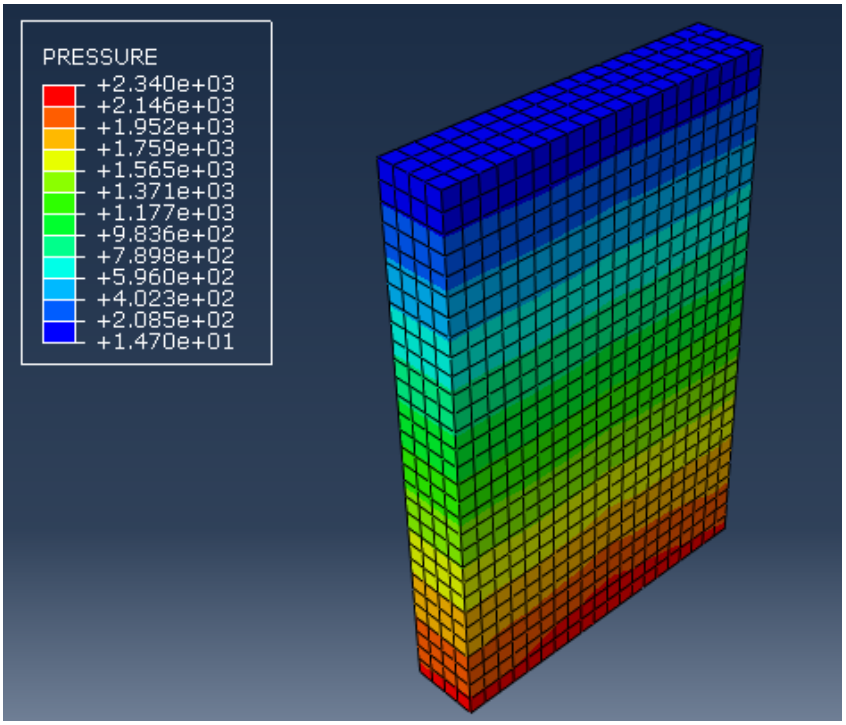

Figure 5: Pressure gradient immediately before divergence for analysis without turbulence defined

Another likely possibility is that the pressure gradient is too large for the CFD module in ABAQUS to model and solve. The large pressure gradient over such a short flow path length, especially given the two phase nature of the flow makes this an extremely difficult problem to solve. To check this assumption a case is run where the pressure gradient is small. With all other inputs remaining the same, instead of a pressure of 2250 psi at the entrance plane, a pressure of 50 psi is defined. This case was run both with and without a turbulence model. The pressure distributions for these cases are shown in Figure 6.

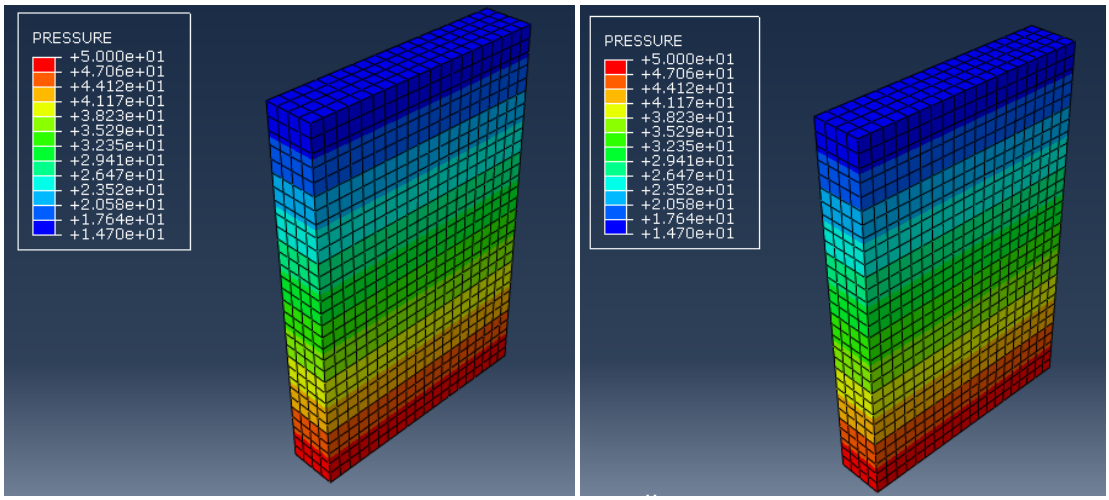

Figure 6: Low pressure gradient results without turbulence (left) and with turbulence (right)

The analysis without a turbulence model defined was able to converge, however the analysis with a turbulence model defined using default parameters was NOT able to converge, even with a small pressure gradient. As a result, the model was enlarged by a factor of 20 to reduce the severity of the pressure gradient, and a very fine mesh was created as shown in Figure 7.

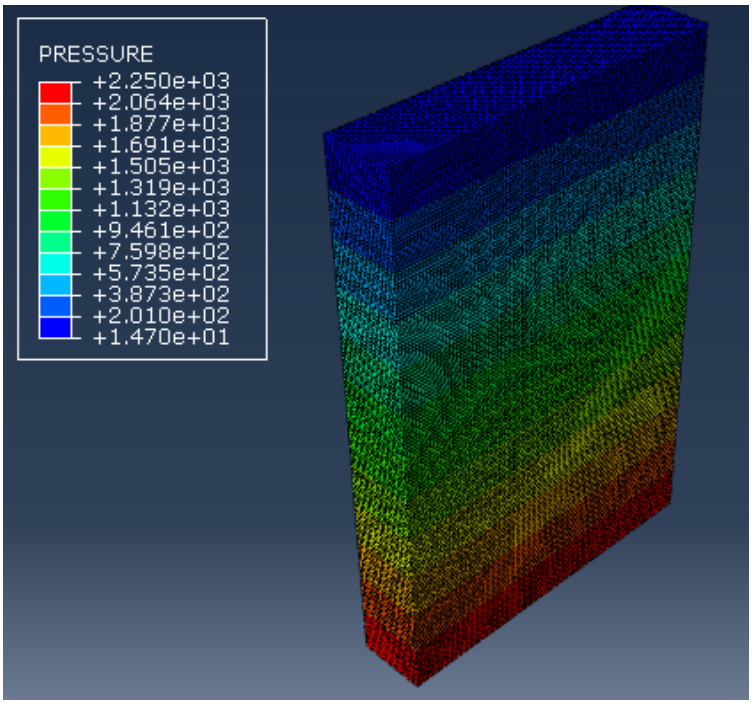

Figure 7: CFD mesh for model scaled 20 times

The first analysis was run without a turbulence model and was able to converge using the larger pressure gradient of 2250 psi. The next analysis added the Spalart-Allmaras turbulence model, using the default

values for the model coefficients. In this analysis the result is not able to converge. In an attempt to obtain convergence, the pressure at the ID was reduced to 250 psi. Although convergence does not occur at the low ID pressure boundary condition, it does come somewhat close, diverging just after 80% of the time step. In order to compare the pressure profile of this case with its laminar flow counterpart, the analysis was run without the turbulence model defined and an ID pressure of 250 psi. Figure 8 compares the pressure gradient for the case with no turbulence model defined and with a turbulence model defined right before convergence and shows that they are exactly the same. Furthermore, it is noted that the pressure drop through the thickness follows a perfectly linear path.

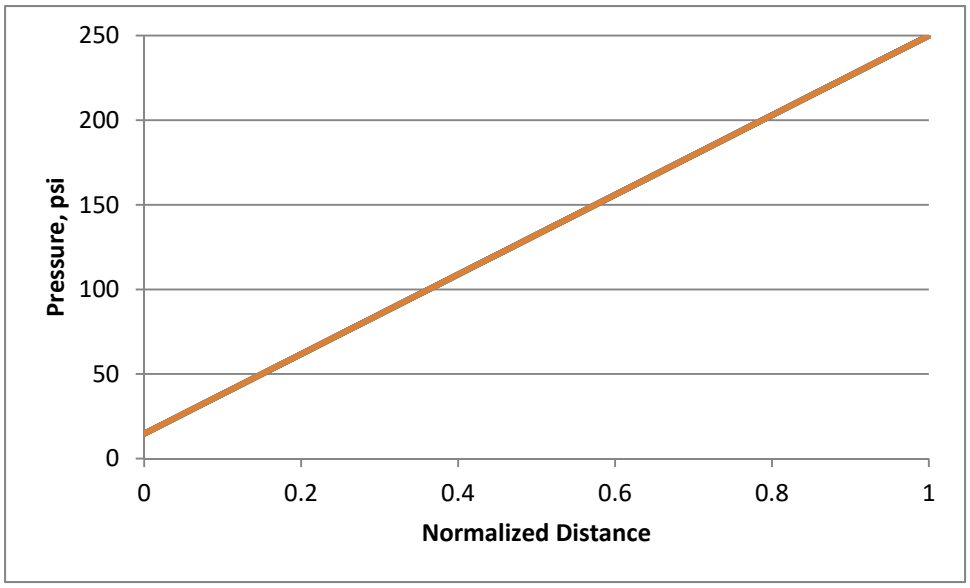

Figure 8: Pressure gradient with and without turbulence model defined.

In actuality, the pressure gradient along the flow path should not be the same for laminar and turbulent flow, and a sharp pressure loss is expected due to entrance effects. Given that the fluid model in this case is simplified to only a single phase with a fixed pressure gradient defined at the entrance and exit planes, the linear pressure gradient along the flow path is reasonable. However to determine if modifications to the turbulence models would impact the pressure along the flow path, the turbulence models that are available in the ABAQUS CFD module, the Spalart-Allmaras model and the k-epsilon model, [1] were looked at more closely. Although the k-epsilon model is more widely used, the default values for the coefficients in ABAQUS are different than what is known as the standard k-epsilon model. Since it is not known if there are differences in the ABAQUS k-epsilon model and the standard k-epsilon model, the analysis was initially run with the k-epsilon model defined using the default ABAQUS values, and the same results were obtained. However, since the ABAQUS values are different than the standard values, it would be recommended to get more insight into why this is the case, and if there are in fact differences between the ABAQUS and standard k-epsilon models. However, given that this model was run with several other pressure definitions at the ID and OD and the results every time showed a perfectly linear pressure distribution across the flow path, it is concluded that the current CFD software that is available is not adequate to address this problem.

3. CFD Problem Statement

Since the CFD software programs currently available are not able to model the problem in a way that meets our needs, representatives from two CFD software companies were contacted to discuss the capabilities and limitations of their programs. Both companies showed interest in looking at the fluid flow through a crack problem to determine if this is a problem they would like to contribute their own resources to and use to expand their capabilities. The problem description for distribution to these companies is described included as Appendix A – CFD Problem Statement. While this option is still under consideration, this line of evaluation was interrupted by the COVID-19 pandemic and is on hold until further notice.

4. Experimental Data

The model that is implemented into the leak rate codes SQUIRT and LEAPOR (which is used in xLPR), is the Henry-Fauske thermohydraulic model [4] [5]. This model is based on a homogeneous flow model for flow through long tubes. The experiments that have been done to validate the model are on larger scales than the small crack sizes that can occur in nuclear piping, especially when looking at low leakage rate crack sizes.

One of the original experimental data sets that was used for the validation of SQUIRT was from the experiments performed by Amos and Shrock [6]. Two figures in that paper show the measured pressure as a function of the distance along the flow path for two of those experiments. Those two figures were digitized, and the digitized information is shown in Figure 9. In both of the curves it looks as though there is an initial pressure drop at the entrance of the crack and then an almost linear decrease, before it finally has a large drop to the exit plane pressure value.

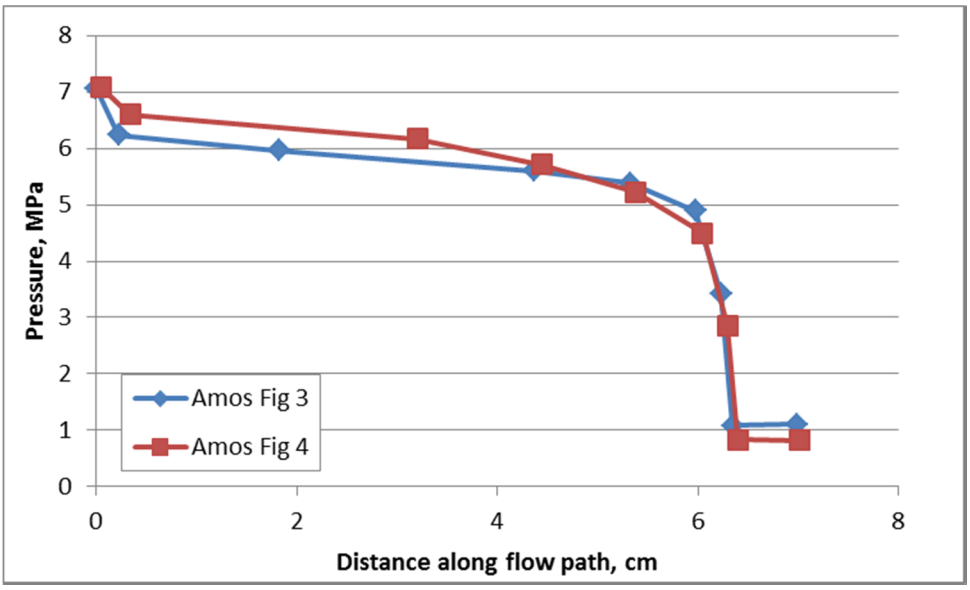

Figure 9: Digitized pressure along flow path in Amos leak rate experiments

The experimental data that the SQUIRT code (and LEAPOR) were validated with are at least 40 years old. It is also known that there have been other leak rate experiments since that time, although they may not have the exact conditions that are applicable to this problem. However, some of these experiments may provide additional insight into the pressure distribution along the flow path. Therefore, a literature study of leak rate experiments and pressure along the flow path of two-phase flow was performed. Some of the studies that were investigated included two-phase flow through microchannels. Many of these studies use refrigerants as the fluid, or a combination of two different fluids existing in different phases, such as air and water. Many of the studies were for fluids experiencing a smaller pressure gradient, or a lower temperature than a fluid flowing through a crack in a nuclear power plant.

Figure 10 shows the relationship between the local pressure drop and Reynolds number and Figure 11 shows the local pressure drop as a function of leak path length divided by hydraulic diameter (L/D) and the fluid velocity determined by Roul and Dash [7]. The hydraulic diameter is defined as $D = \frac{4A_o}{P_w}$ where A_o is the area at the crack entrance and P_w is the wetted perimeter of the flow area. The step decrease in Figure 11 at L/D = 0 is due to an orifice that it placed in the pipe.

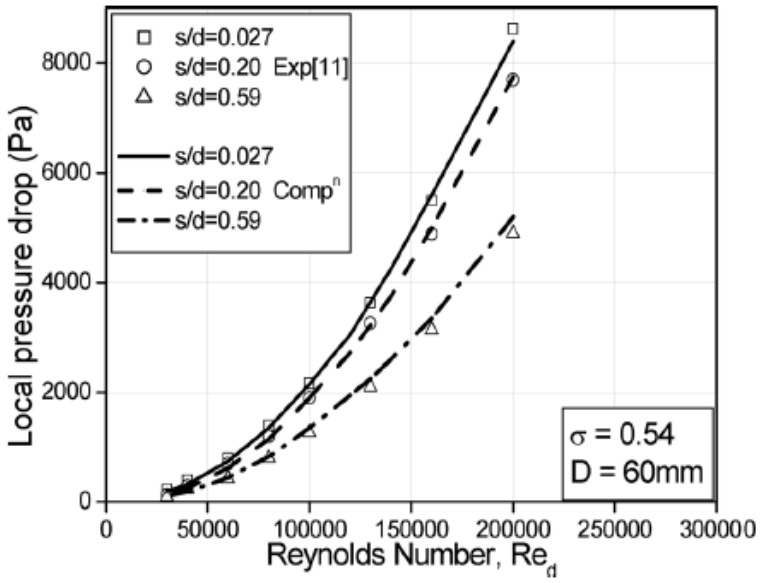

Fig. 14 Single-phase pressure drop as a function of local Reynolds number for $\sigma = 0.54$

Figure 10: Roul and Dash relationship between local pressure drop and Reynolds number

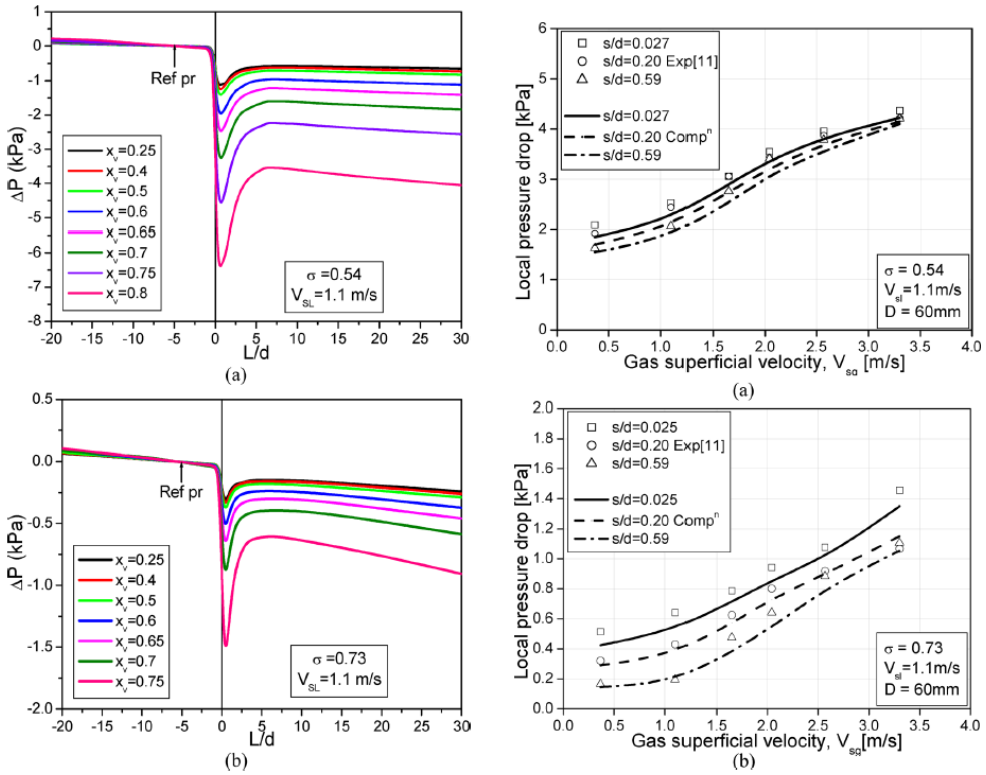

Fig. 15 Pressure profiles for two-phase air-water flow through $D = 40$ mm, $s/d = 0.2$, (*a*) $\sigma = 0.54$, (*b*) $\sigma = 0.73$ orifice

Fig. 16 Local pressure drop as a function of gas superficial velocity and orifice thickness (*a*) $\sigma = 0.54$, (*b*) $\sigma = 0.73$

Figure 11: Roul and Dash pressure drop as a function of L/D (left) and gas velocity (right)

Although the fluid in this experiment is an air and water mixture, these relationships can be used to gain insight to the two phase water-vapor mixture that is found in nuclear applications.

Other experiments that use a water-vapor mixture as the fluid, such as those of Ghosh [8], and Vadlamani and Revekar [9], show that tighter slits or short flow path lengths have different flow behavior than those with larger openings or long flow paths. This is important because the Henry-Fauske model that the current leakage rate software codes are based on has an assumption that the flow path is long, and in fact must have an L/D ratio of at least 12 where a choke plane and choked flow are assumed to exist. Choked flow is a limiting condition where the mass flow will not increase with a further decrease in the downstream pressure environment for a fixed upstream pressure and temperature.

The most promising result of the literature study is a paper by De Lorenzo [10], et al, titled "Benchmark of Delayed Equilibrium Model (DEM) and classic two-phase critical flow models against experimental data." This paper compares the Henry-Fauske model (which is the thermohydraulic model that is used to calculated the leakage rate in xLPR), the Homogeneous Equilibrium Model (HEM), the Delayed Equilibrium Model (DEM), and the Moody model with the experimental data from the Super Moby Dick experiments. The Super Moby Dick experiments were performed by the CEA-Grenoble and consisted of two-phase critical flashing flow experiments. Steady state critical flow conditions were measured in a long nozzle and in a short nozzle. The long nozzle had an elliptic convergent section at the entrance

followed by a straight pipe of about 0.5 m long and of 20 mm inner diameter and ended by a 7° divergent section. The short nozzle had the same geometry without the divergent section. Twelve reference tests were chosen for each nozzle for four different pressures at the inlet: 20, 40, 80 and 120 bar (2, 4, 8 and 12 MPa). For each pressure, three different temperatures were tested. The water was subcooled or quasi-saturated at the inlet of the nozzles. The results from these experiments are in shown in Figure 12.

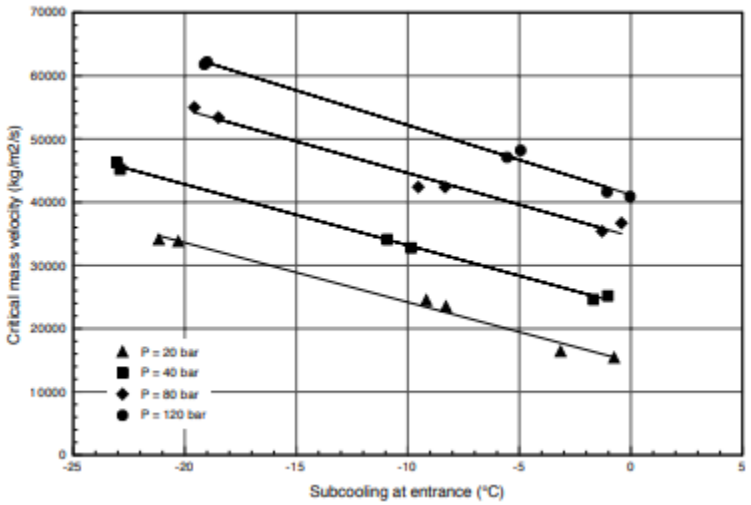

Figure 12: Evolution of critical flow rate for Super Moby Dick experiments

Many of the experiments by which the leakage rate codes, such as SQUIRT and LEAPOR, have been validated, report the flow rate and pressure at the entrance and exit of the flow path, but not at points along the path. The Super Moby Dick experiments however do record the pressure at different points along the flow path. The paper by De Lorenzo et al compares the pressure along the path the DEM model prediction. One of the figures in this paper (Figure 13) shows that the DEM model is in very good agreement with the Super Moby Dick measurements.

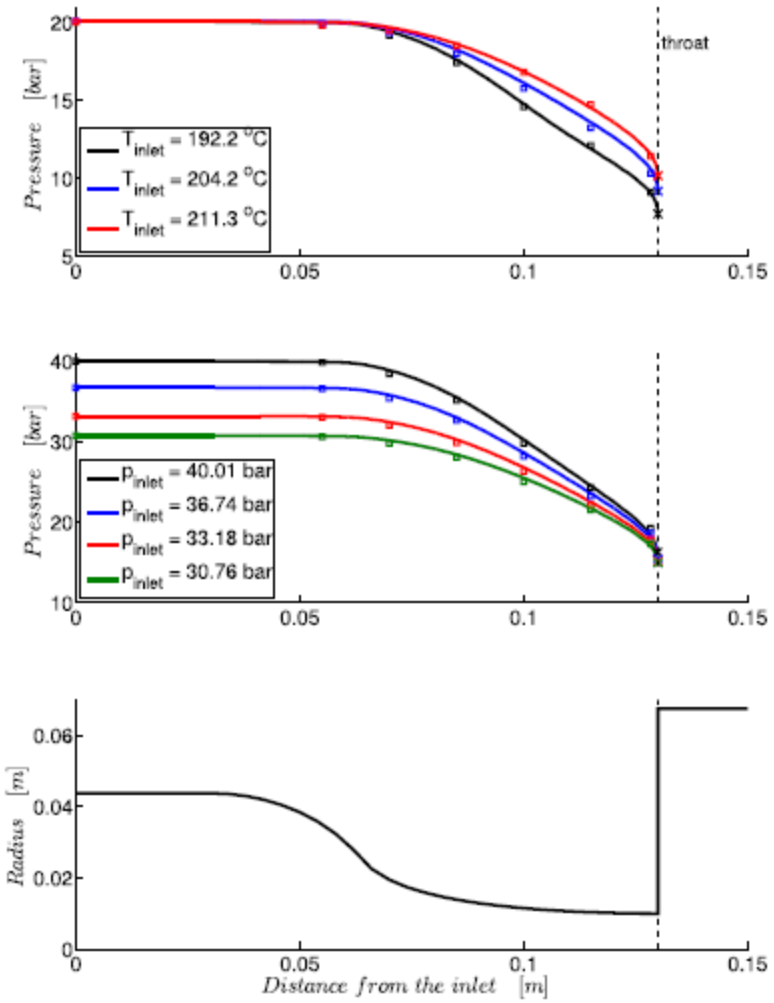

Fig. 9. At the top, there is the pressure profile in SMD short test section for $p_0 = 20$ *bar*. In the central plot, the pressure profiles of four tests at $T_0 = 234$ °C is depicted. At the bottom, we report the geometry of the test section. Solid lines indicate the simulation results of DEM, instead, square markers □ represent the experimental measurements of Jeandey and Gros D'Aillon (1983). The locations of the critical section are depicted with the marker × and, practically, coincide with the throat. From the plot on the top the trend is quite clear: the higher the subcooling, the stronger is the pressure decrease in the nozzle. Instead, from the central plot, we can see that the critical pressure, in short nozzles, seems to be not affected by the stagnation pressure. The dominant role is played by the stagnation temperature.

Figure 13: Pressure Profile from Figure 9 of De Lorenzo paper

This paper also compares the leakage rate and the critical pressure predictions from the Henry-Fauske model, Moody model, HEM, and DEM to the experimental predictions. Comparison of the Henry-Fauske model predictions with Super Moby Dick measurements are shown in Figure 14, below.

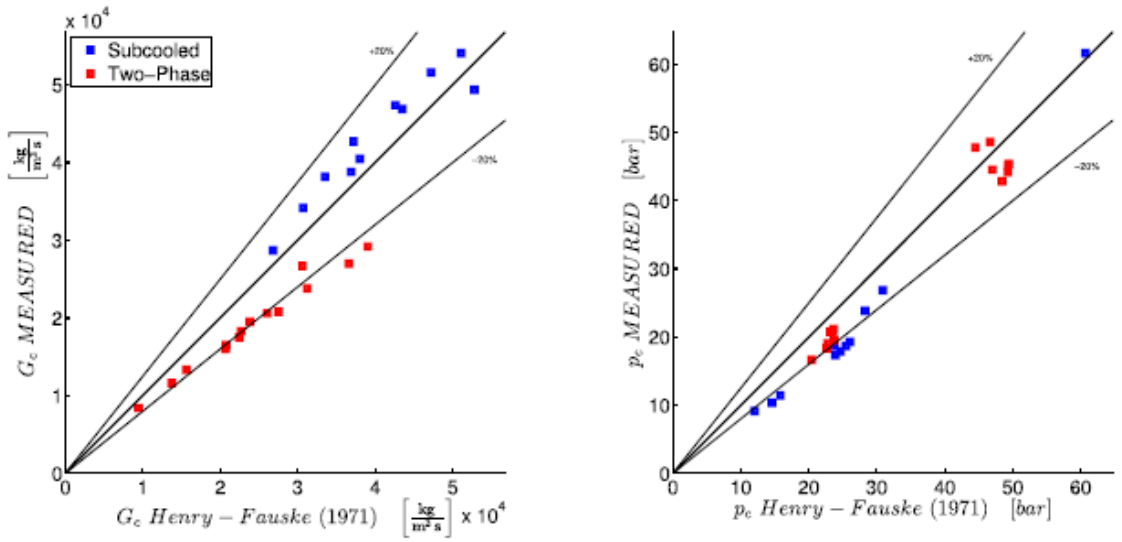

(a) Henry-Fauske model (1971)

(a) short tubes

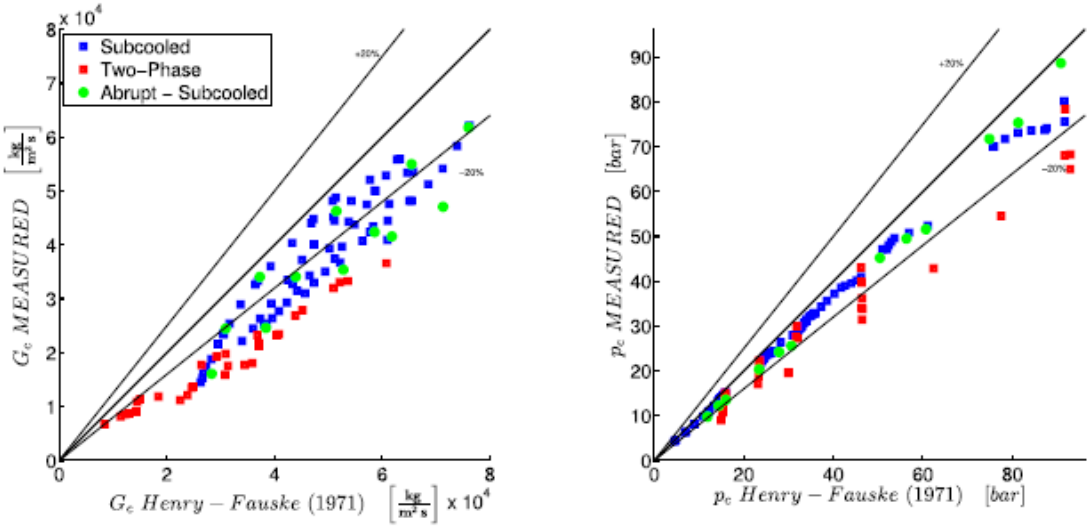

(a) Henry-Fauske model (1971)

(b) long tubes

Figure 14: Comparison of Henry-Fauske model predictions of flow rate and critical pressure to Super Moby Dick tests using (a) short tubes and (b) long tubes

Leak Rate experiments were also performed by Yang, et al [11], for high pressure and temperature flows through a simulated crack. One figure from this report (shown below in Figure 15) also shows pressure measurements at different points along the flow path.

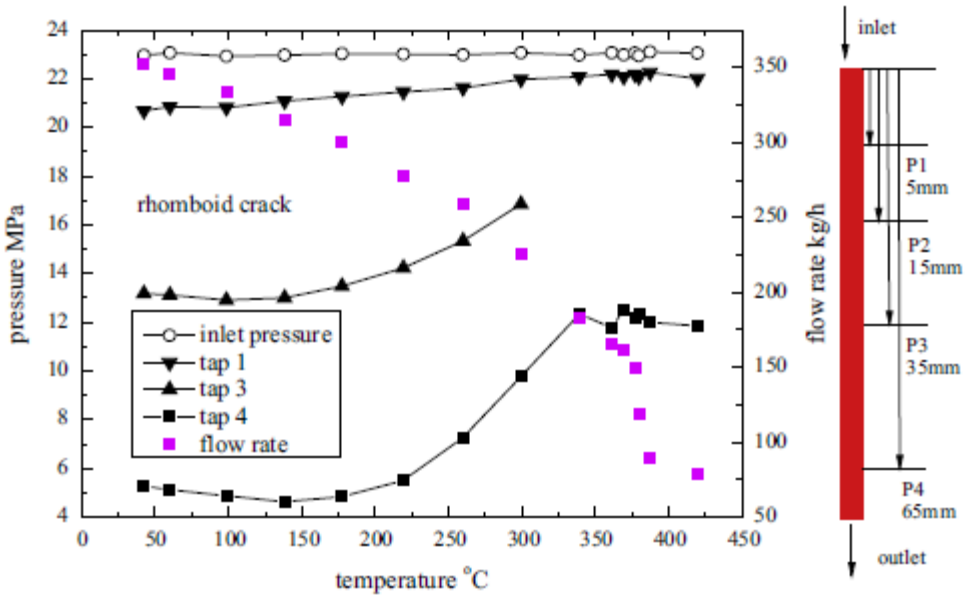

Figure 15: Pressure distributions at different measuring positions for Yang, et al experiments

The DEM model that was introduced in the De Lorenzo paper was looked at more closely. This model provides an analytical solution that matches well with the experimental data included in the paper, as shown in Table 2 and Figure 16.

Table 2: Mean Error for Critical Mass Calculations

	HEM	Moody	Henry–Fauske	DEM
Two-phase inlet				
SMD long	−0.0064	0.7047	0.6455	0,0603
SMD short	−0.1565	0.4275	0.2511	0,1748
Environmental	−0,1226	2,0749	0,4679	−0,1040
Subcooled inlet				
SMD long	−0.0584	0.0892	0.3162	−0,0186
SMD short	−0.3625	−0.2277	−0.0705	0,0574
John et al. (1988)	2.1699	2.3201	2.5422	0.0096
Environmental	0,0405	0,0335	0,4875	−0,0144
Sozzi-Sutherland (1975)	0,0342	0,1449	0,3679	0,0568
Ardron-Ackerman (1978)	−0,4864	−0,2747	−0,0589	−0,0478
Boivin (1979)	0,0102	0,1973	0,5100	−0,0597
Seynhaeve (1980)	−0,4636	−0,3428	−0,1076	−0,0004
BNL (1981)	−0,2048	−0,2340	0,0014	−0,0105
STEP	−0,2089	−0,3272	−0,1092	0,0169

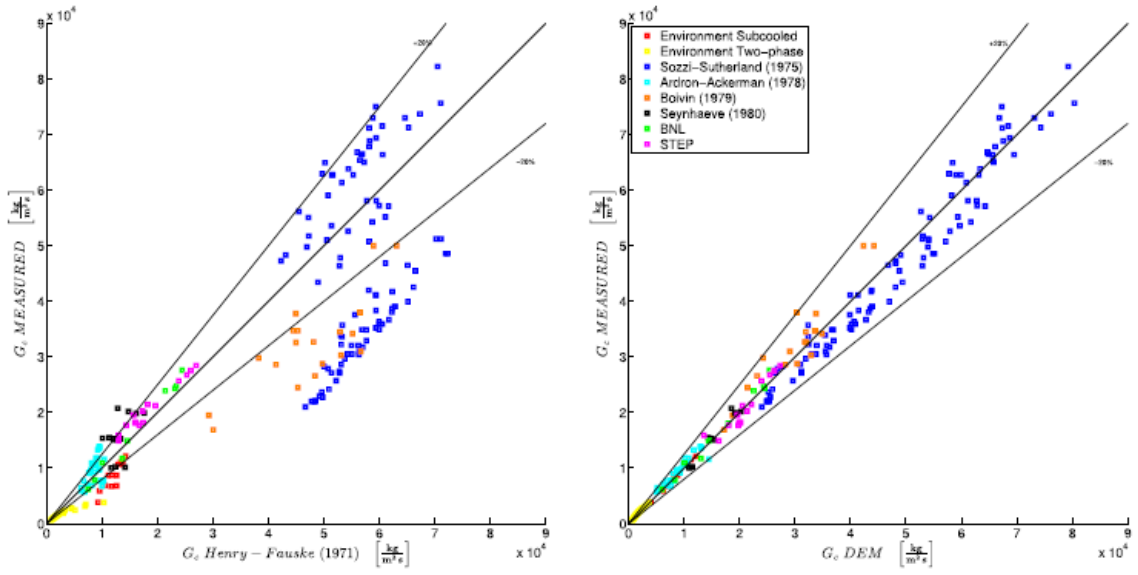

(a) (b)

Figure 16: Henry-Fauske (a) and DEM (b) predictions of critical mass flux compared to experimental data

Based on the information in Table 2 and Figure 16, the DEM model is a good candidate to pursue in order to develop the pressure along the flow path relationship.

The experimental data presented in this section shows a general trend of an initial entrance loss pressure drop, and then an almost parabolic drop to the pressure at the outer diameter crack plane. Using this information, a generic curve of this pressure drop can be modeled and applied to the crack face pressure in a finite element analysis. This is described in the following section.

5. Finite Element Analysis

In order to assess the impact of the crack face pressure on the COD and resulting leakage rate, a finite element model of a nominal sized hot leg with a though wall crack was generated. In xLPR the assumption is that the crack face pressure is half of the internal pressure. To assess the impact of this assumption for the pressure distribution on the crack face, three pressure profiles are applied to the crack face for three different crack sizes, and the resulting CODs and leak rates are compared. The geometry of the hot leg pipe and the loads are listed in Table 3. It is noted that the axial load consists only of the pressure induced axial stress and does not include any bending moment.

Table 3: Hot Leg Geometry and Loads

Inside Diameter (in)	29.0
Thickness (in)	2.45
Axial Load (ksi)	7.221
Internal Pressure (psi)	2250

Each of these pressure profiles that were applied to the crack face are shown graphically in Figure 17. The analysis labeled uniform consisted of a uniform, constant pressure of one half the internal pressure, or 1125 psi. The analysis labeled linear consisted of a pressure profile that decreased linearly over the crack face, from the inner diameter to the outer diameter. Finally, the analysis labeled model consisted of a pressure profile that was approximated based on the experimental results shown in Section 4.

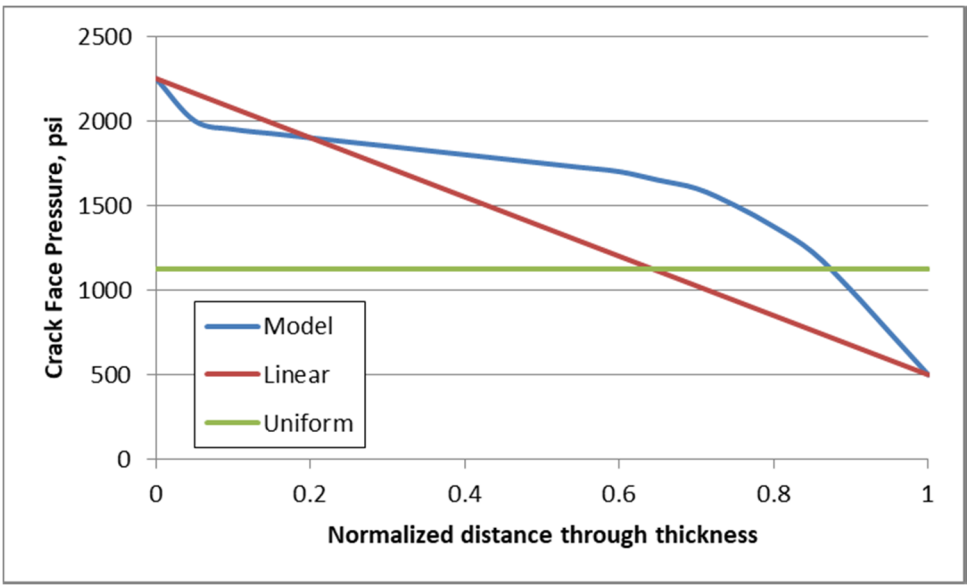

Figure 17: Pressure profiles used in FEA

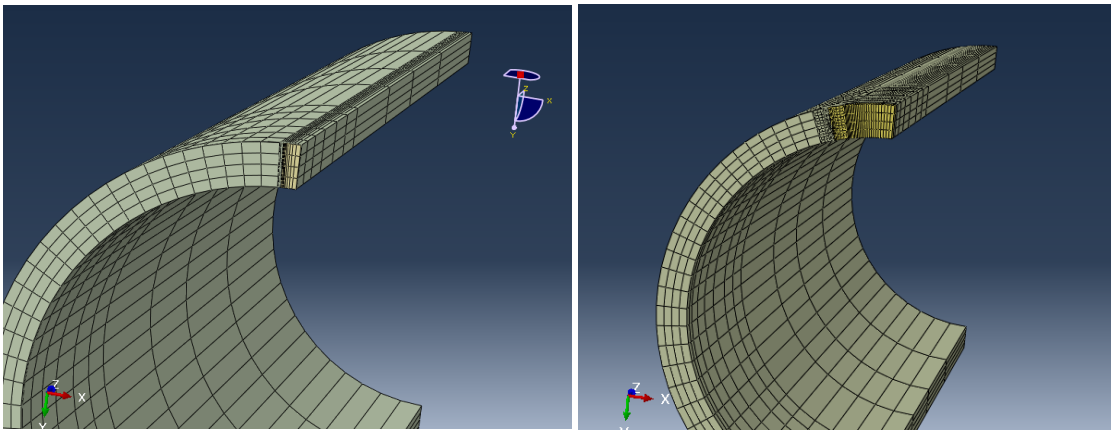

(a) **(b)**

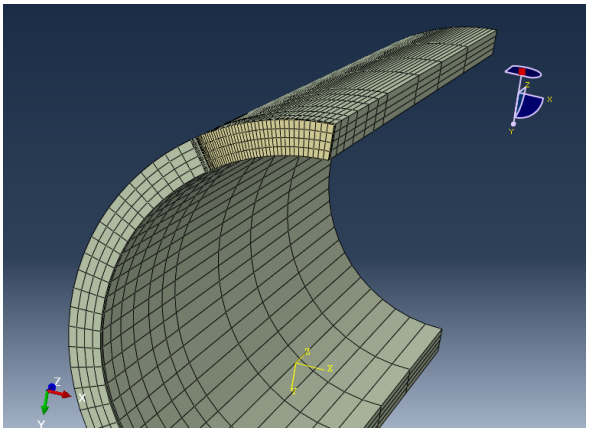

(c)

Figure 18: Mesh for c=1.0 (a), c=5.0 (b) and c=10 (c)

Figure 18 shows the crack mesh for the three crack sizes that were analyzed: 2.0 inches, 10.0 inches and 20.0 inches. The ABAQUS analysis gives the results for the COD at points along the flow path. The inner diameter, outer diameter and mid-thickness values were recorded, and these values were used as input to LEAPOR for leak rate calculations. The COD values for the 2.0 inch crack are listed in Table 4, the COD values for the 10.0 inch crack are listed in Table 5 and the COD values for the 20.0 inch crack are listed in Table 6.

Table 4: COD for 2.0 inch crack

Pressure Distribution	ID COD (in)	Mid COD (in)	OD COD (in)
Uniform	1.18E-03	1.13E-03	1.38E-03
Linear	1.32E-03	1.16E-03	1.30E-03
Model	1.26E-03	1.16E-03	1.30E-03

Table 5: COD for 10.0 inch crack

Pressure Distribution	ID COD (in)	Mid COD (in)	OD COD (in)
Uniform	5.83E-03	6.83E-03	7.94E-03
Linear	6.30E-03	7.06E-03	7.94E-03
Model	6.37E-03	7.27E-03	8.23E-03

Table 6: COD for 20.0 inch crack

Pressure Distribution	ID COD (in)	Mid COD (in)	OD COD (in)
Uniform	1.92E-02	2.30E-02	2.69E-02
Linear	2.05E-02	2.42E-02	2.80E-02
Model	2.99E-02	3.42E-02	3.86E-02

LEAPOR is the leakage calculation code that is used within xLPR, and was therefore the program that was used to calculate the leak rates using the COD values from the above calculations. LEAPOR allows for different values of the COD on the ID and OD to be input, however, it determines an equivalent COD from those inputs, which it then uses to calculate the leak rate. Therefore, the leak rate calculations were performed for four different COD inputs: using the FEA Mid-thickness value as the input for both the ID and OD, using the FEA ID value as the ID input and the FEA OD value as the OD input, using the FE ID value as the input for both the ID and OD, and using the FE OD value as the input for both the ID and OD. The leak rates calculated using these detailed are shown in Table 7 for the 2.0 inch, Table 8 for the 10.0 inch crack, and Table 9 for the 20.0 inch crack.

Table 7: Leak Rates for 2.0 inch crack

	Leak Rate (gpm)			
Pressure Distribution	ID-OD	Mid only	ID only	OD only
Uniform	0.04315709	0.03218702	0.03511223	0.04761239
Linear	0.04319548	0.03403726	0.04372794	0.04298646
Model	0.04189968	0.03372016	0.03997545	0.04266526

Table 8: Leak Rates for 10.0 inch crack

	Leak Rate (gpm)			
Pressure Distribution	ID-OD	Mid only	ID only	OD only
Uniform	1.94186138	1.93191596	1.61043596	2.30552846
Linear	2.02860172	2.00866045	1.76100695	2.30418312
Model	2.08671292	2.07941903	1.78269447	2.40424032

Table 9: Leak Rates for 20.0 inch crack

	Leak Rate (gpm)			
Pressure Distribution	ID-OD	Mid only	ID only	OD only
Uniform	21.36036247	19.22066958	14.3719635	25.6353955
Linear	23.56612168	21.03272538	15.9342894	27.86556522
Model	56.58647199	47.72902774	32.25551892	65.91550438

There are a couple of important notes about the leak rate results. The first is that for the 2.0 inch crack, when using the mid-thickness COD as the input for both the ID and OD COD, the linear and model pressure distribution CODs lead to an increase in the calculated leak rate. However, when using the FEA ID and OD COD as the respective LEAPOR inputs, the linear and model pressure distributions lead to a decrease in the calculated leakage rate as compared to that from the uniform pressure. This is an interesting result that should be investigated further, however, it is outside the scope of this study. The second note is that the model pressure distribution has a much more significant impact on the calculated leak rate for the longer crack size. This is expected since the COD determined by the FE analysis is over 2 times higher than when a uniform or linear distribution is used. This result should be used with caution however. The model pressure distribution is based on a general trend of what has been seen in past experiments but is not based on the physics of this particular problem. In other words, the distribution may be more accurate for smaller crack sizes, but a modification should be made for larger crack sizes. Regardless, what is consistent with both the small and long crack sizes, is whatever the correct pressure distribution should be is important in predicting accurate leakage rates. Even the difference between the model and linear pressure distributions is significant for both crack sizes verifying the importance of this input on the calculated CODs and their associated leak rates.

To more clearly see the impact of the pressure distribution on the calculated leak rates the percent difference is detailed in Table 10 for the 2.0 inch crack,

Table 11 for the 10.0 inch crack, and Table 12 for the 20.0 inch crack.

Table 10: Percent Difference for 2.0 inch crack

	% Difference with Uniform			
	ID-OD	Mid only	ID only	OD only
Linear	0.08891%	5.58780%	21.85614%	10.21190%
Model	2.95664%	4.65242%	12.95344%	10.95981%

Table 11: Percent Difference for 10.0 inch crack

	% Difference with Uniform			
	ID-OD	Mid only	ID only	OD only
Linear	4.36928%	3.89509%	8.93214%	0.05837%
Model	7.19121%	7.35431%	10.15337%	4.19179%

Table 12: Percent Difference for 20.0 inch crack

	% Difference with Uniform			
	ID-OD	Mid only	ID only	OD only
Linear	9.81942%	9.00324%	10.31025%	8.33693%
Model	90.38496%	85.16352%	76.70822%	87.99500%

Given these results, the assumption currently implemented that the pressure distribution is uniform with a value half of the internal pressure has a significant impact on the COD, and thus the calculated leakage rate, especially as the crack length increases, and at leakage rates between 1gpm and 10 gpm. Accurate leakage predictions ultimately impact the leak-before-break analysis and calculated probabilities of rupture with leak detection. Therefore, more accurate predictions of the pressure on the crack face is suggested as an improvement to the xLPR code.

6. Future Considerations

As Sections 2 and 3 show, the fluid flow through a crack in nuclear piping where the water flashes to steam, creating a two-phase mixture, is an extremely complex problem to solve, and one in which current CFD software codes cannot solve without making simplifications. Although these model or input simplifications will impact the results, it is unknown what that impact will be. Therefore, having experimental data by which to validate any models is very important. The experimental data that was used to validate current leakage rate software codes have shortcomings that include the fact that most were for flow though slits rather than flow through cracks. Furthermore, all were for long flow path lengths which ensured the fluid was in a state in which the Henry-Fauske model was valid, and most of the experiments did not measure the pressure along the flow path. Additionally, the experiments did not adequately measure the crack morphology and its impact on the leak rate, if it was accounted for at all. The knowledge that has been obtained on factors that influence the leak rates, such as pressure along the

crack face (impacting COD), and crack morphology (impacting the pressure) can be used to design experiments that better measure the properties of interest, and provide more modern model validation.

Of the experiments discussed in Section 4 that did measure the pressure along the flow path, the data is limited, but shows a general trend. This general trend seems to be able to be reproduced using the Delayed Equilibrium Model (DEM) presented by De Lorenzo et al. Additionally, as the comparisons in the De Lorenzo paper show, the DEM model gives better predictions of the experimental leak rates than the Henry-Fauske model does. Therefore, it is worthwhile to consider studying this model more in depth and considering using the DEM model in place of the Henry Fauske model for leak rate calculations.

Finally, the current available models in the CFD software codes that were investigated do not have the capability of solving the problem of two phase flow through a crack in its entirety due to the complex nature of the fluid, its changing properties, and the small-scale, rough, tortuous flow path. Yet, one of the benefits of CFD is that if an adequate model did exist to solve this problem, then it is much easier, and less costly, to get more data and study different effects. Some of these effects include, the crack opening shape, the roughness, the path tortuosity, and the flow path length, among others. Additionally, data can be obtained about the pressure, temperature, quality, and other fluid properties, from every point in the mesh if desired. Furthermore, the CFD framework provides a test bed for optimization of a model to better match experimental results.

Appendix A – CFD Problem Statement

Background

The Leak Before Break (LBB) concept uses the leakage detection capability to determine the size of a through wall crack that can be detected, and then performs a stability analysis on this crack size. Most research related to LBB applications has focused on the initiation and propagation of cracks. New generation commercial power plants, other unique reactors, as well as LBB being applied in other fields such as space vehicle tanks, transport pipelines and offshore installation, and the advanced capabilities of leak-detection systems, have made the ability to accurately predict the leakage through a narrow crack an increasingly important issue. When the LBB concept was initially applied to nuclear power plants, the leakage detection technical specification was typically 1 gpm, and a safety factor of 10 was applied to this limit. Therefore, the target leakage was 10 gpm. As leakage detection capabilities have improved, and as probabilistic codes have increasingly been used to determine rupture probabilities, the target leakage can be as low as 0.001 gpm, or 4 orders of magnitude lower. There are several complications that arise with leak rates this low.

When looking at the compilation of the predicted to experimental leak-rate test data, the scatter is increasingly larger at the lower leak-rates (see Figure 19). The lower leak-rate test data were generated during IGSCC cracked pipe tests done at Battelle. At that time (~1984), it was not known how to properly characterize the crack morphology so all pressure drop terms were thrown into a single "roughness" value determined from measurements on the test specimen fracture surfaces made in a machine shop. The majority of leak-rate test data used specimens with randomly created roughness's on each side where there are not mating peaks and valleys like for natural cracks. A multitude of metallographic sections of service cracks have been made (See NUREG/CR-6004), that allows one to extract some crack morphology parameters for different service-degradation mechanisms, but these measurements of the crack morphology were determined in one plane, with the 3D nature of the cracks ignored. Additionally, the measurements were subjective since there were no defined procedures nor guidelines. This leak-rate experimental effort was done before any leak rate codes were developed.

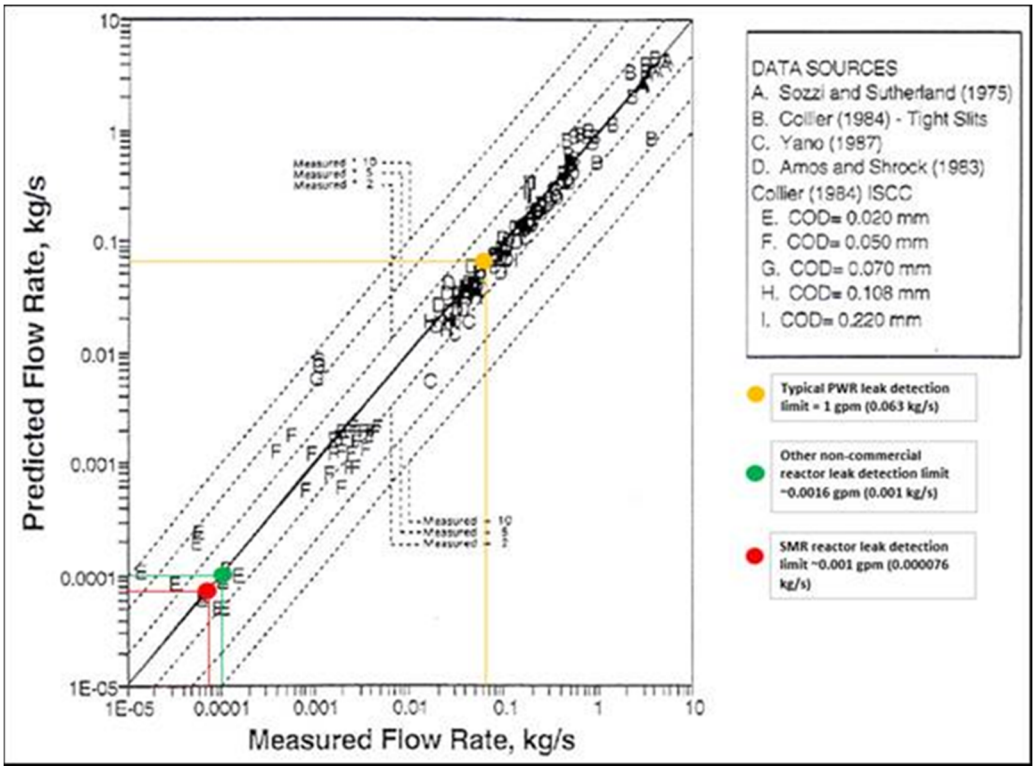

Figure 19: Predicted (from SQUIRT) versus experimental leak-rates for subcooled water tests showing increased scatter at lower leak-rates (from NUREG/CR-6861, 2004)

We currently understand that there are four crack morphology parameters; (1) entrance/exit plane sharpness, (2) surface roughness, (3) number of 90-degree turns, and (4) flow path length/thickness. However these values can change depending on the crack-opening displacements, so local parameters are applied when the crack is tight, and global parameters are applied with the crack opening which is much larger than the global roughness. The relationship on the transition of the local to global crack morphology parameters depends on engineering judgment, and not any validated leak-rate data or CFD analyses. There has been some CFD work by Bagshaw [12] that confirms there is a COD dependency of the crack morphology parameters (see Figure 20 below), but the cracks were idealized shapes not tortuous SCC cracks where there are not idealized 90-degree turns.

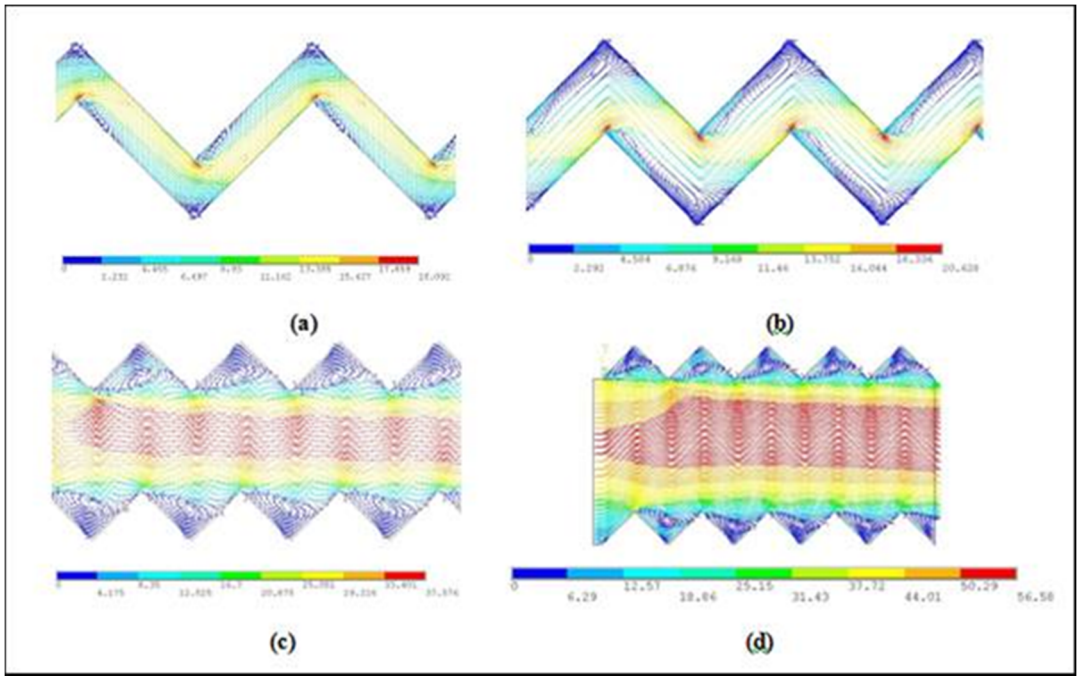

Figure 20: CFD analyses for simple crack roughness models showing how the crack-opening area affects the flow behavior (NUREG/CR-6861, 2004) (a) COD/roughness = 0.5; (b) COD/roughness = 1.0; (c) COD/roughness = 3.0; (d) COD/roughness = 5.0; with subcooled water at PWR conditions

The smaller the leakage rate, the smaller the crack opening area is, leading to very narrow cracks. Flow through narrow cracks involves very complex thermal-hydraulic phenomena, in addition to the rough surfaces and turning flow path that is not encountered in channel or artificial slit flow. The non-uniform flow path and narrow crack opening can lead to blockage in some cases. The current thermal-hydraulic models are based on flow through smooth channels, with modifications to the pressure loss terms to attempt to account for the crack morphology parameters mentioned above. Even without the added complication of the crack path tortuosity, the thermal-hydraulic phenomena that the fluid undergoes in current LBB applications are complex. The fluid begins as a single phase liquid, and then undergoes phase transformation to become a two-phase liquid/gas choked flow. The transformation from a single phase to two-phase fluid is dependent on several parameters including the pressure, temperature, and the length to diameter (L/D) ratio among others.

The crack morphology parameters are dependent on the material, and the way that the crack was initiated. In current nuclear power plant applications, the cracks are classified as air fatigue, corrosion fatigue, primary water stress corrosion cracking (PWSCC), or intergranular stress corrosion cracking (IGSCC). Each of these cracking mechanisms has different average values for the roughness, number of turns and path deviation. However, even within a cracking mechanism, there is a wide range of measured values for each of the morphology parameters, due to various factors such as material variability, applied stress, and the subjectivity of the person performing the measurements. Since the effect of the crack morphology is applied as a pressure loss, these parameters have a significant effect on the calculated leak rate.

Problem Statement

In order to address some of the issues and complications discussed above, the proposed concept includes both experimental and computational components. The experimental component would consist of making 3D replicates of service-induced cracks for leak-rate testing. Actual fracture surfaces can be optically scanned to get a digital file of the fracture surface for 3D printing. There are now much improved optical microscopes for metallographic measurement, which are capable of scanning a fully focused, high-accuracy digital 3D map of a fracture surface by seamless 3D image stitching. One optical system [13] that has been explored has a capability of measurements with spacing of 1.0 micron along the horizontal X-Y coordinates of a fracture face and that can follow fracture surface contours with 0.1 microns resolution in the vertical Z-direction. The 3D map of the fracture surface (with some additional file manipulations) that is generated by the microscope would then be used to manufacture mating surfaces by 3D printing with a metal material. The 3D printing has less resolution than the optical measurements at this time but is still smaller than the global roughness (and the 3D printing resolutions are constantly improving); hence the optical/digital measurements are not limiting. Using the latest 3D printing techniques with fine metallic powders, test samples can be consistently replicated with dimensions and patterns of our choice. These 3D printed blanks can then be put in a secured blind flange with an adjustable crack opening. Leak rates could be measured with subcooled water, steam, and potentially other fluids. This type of blind flange vessel leak rate testing is illustrated in Figure 21 to Figure 23 (as was used in the earlier EPRI and NRC/IPIRG leak-rate testing projects). This also allows for the ability to change the crack opening distance by separating the test samples at varying distances using different sized spacers. Since the test samples would be printed in this way it would be very easy to recreate the test and run multiple test cases.

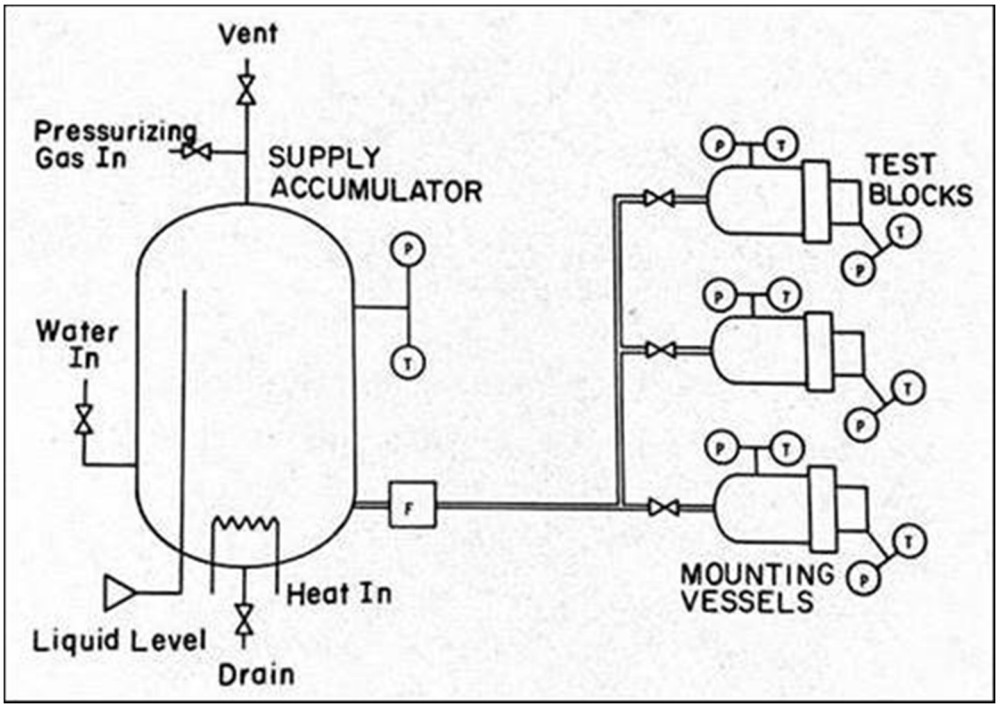

Figure 21: Schematic of leak-rate test facility (EPRI NP-3540-LD, 1984)

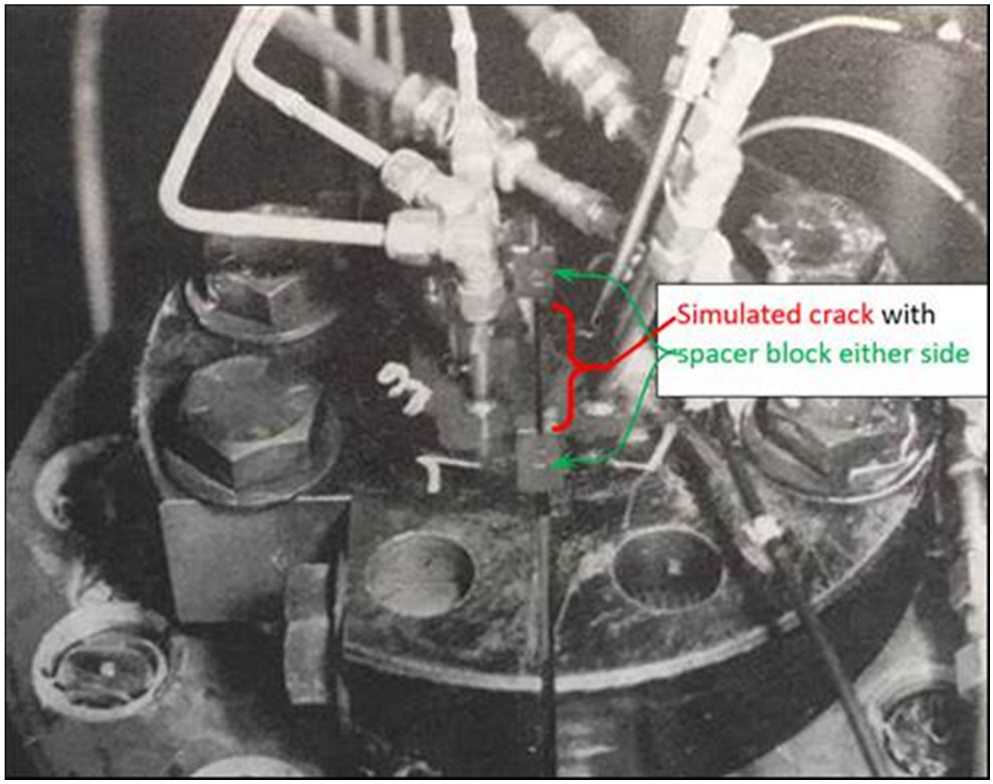

Figure 22: **Simulated cracks inserted in flange for leak rate testing [14]**

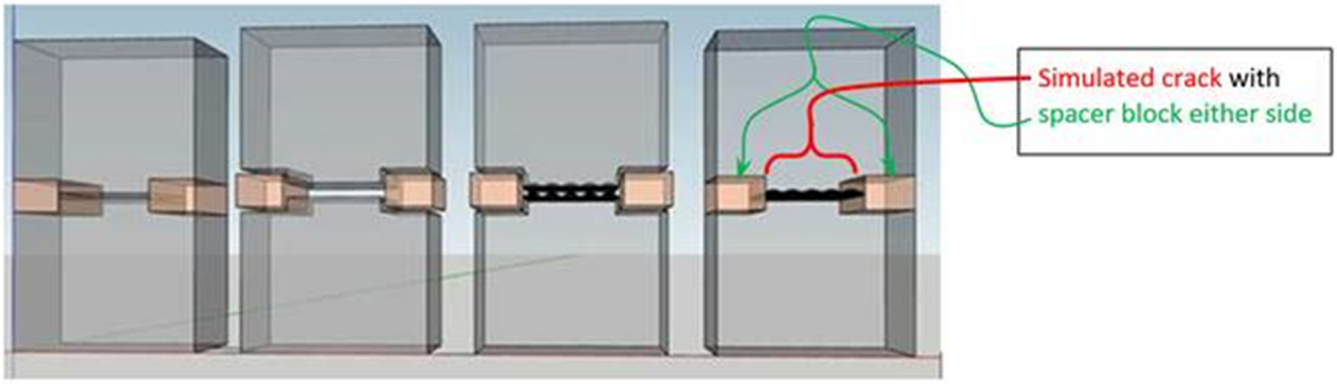

Figure 23: Schematic of using 3D printed natural cracks in test blocks for leak-rate testing

Since the 3D printing process requires an STL file in order to generate the information needed for printing, this same file can be imported into a CFD software program to create the boundary conditions for the fluid flow. The experimental results can be used to validate the CFD analysis, and then the CFD

analysis can be used to further expand the analytical leak rate models by investigating different crack morphology combinations, changing the L/D ratio, the crack opening distance, pressure, temperature, etc.

The resolution necessary from the 3D printing process may not yet be available, and it may be some before that is the case. In the meantime, the process of using a mesh surface that could, at some point in the future, be used to generate a crack surface via 3D printing can still be followed for creating the mesh and setting up the CFD analysis. The CFD analysis can use the currently available leak rate test data for validation. Due to the ease of changing the properties, mesh, and other model parameters, CFD can be used to optimize, or create new, a leak rate model.

References

[1] Simulia, "Abaqus Analysis User's Guide," 2016. [Online]. Available: http://ivt-abaqusdoc.ivt.ntnu.no:2080/v2016/books/usb/default.htm?startat=pt03ch06s06aus49.html.

[2] Engineering Toolbox, "Specific Heat Capacity of Water," [Online]. Available: https://www.engineeringtoolbox.com/specific-heat-capacity-water-d_660.html.

[3] Engineering Toolbox, "Water Viscosity," [Online]. Available: https://www.engineeringtoolbox.com/water-dynamic-kinematic-viscosity-d_596.html.

[4] R. E. Henry, H. K. Fauske and S. T. Comas, "Two-Phase Critical Flow at Low Qualities Part I: Experimental," *Nuclear Science and Engineering,* vol. 41, pp. 79-91, 1970.

[5] R. Henry, "The Two-Phase Critical Discharge of Initially Saturated or Subcooled Liquid," *Nuclear Science and Engineering,* vol. 41, pp. 79-91, 1970.

[6] C. N. Amos and V. E. Schrock, "Two-Phase Critical Flow in Slits," *NUCLEAR SCIENCE AND ENGINEERING,* vol. 88, pp. 261-274, 1984.

[7] M. K. Roul and S. K. Dash, "Single-Phase and Two-Phase Flow Through Thin and Thick Orifices in Horizontal Pipes," *Journal of Fluids Engineering,* vol. 134, pp. 1-14, September 2012.

[8] S. Ghosh, D. Mukhopadhyay and S. Saha, "An experimental analysis of subcooled leakage flow through slits from high pressure high temperature pipelines," *International Journal of Pressure Vessels & Piping,* Vols. 88(8-9), pp. 281-289, 2011.

[9] R. A. Vadlamani, S. T. Revankar and J. R. Riznic, "Theoretical and Experimental Investigation of Subcooled Flashing Flow through," *Heat Transfer Engineering,* vol. 40:7, pp. 524-536, 2019.

[10] M. De Lorenzo, P. Lafon, J.-M. Seynhaeve and Y. Bartosiewicz, "Benchmark of Delayed Equilibrium Model (DEM) and classic two-phase critical flow models against experimental data," *International Journal of Multiphase Flow,* vol. 92, pp. 112-130, 2017.

[11] Z. Yang, Q. Bi, G. Zhu and e. al., "Leak rates of high pressure steam–water across," *Experimental Thermal & Fluid Science,* vol. 59, pp. 118-126, 2014.

[12] N. Bagshaw, "A Study of Leak Rates Through Narrow Cracks," The University of Sheffield, PhD Thesis, Department of Mechanical Engineering, September 2000.

[13] Keyence, "4K Ultra-High Accuracy Digital Microscope," [Online]. Available: https://www.keyence.com/ss/products/microscope/pr_vhx-7000/.

[14] EPRI, "Two-Phase Flow Through Intergranular Stress Corrosion Cracks and Resulting Acoustic Emission," 1984.